[90] Y. Kobayashi and S. Yoshida, "Bandpass filters using TM_{010} dielectric rod resonators," in *1978 IEEE MTT-S Int. Microwave Symp. Dig.*, pp. 233–235, June 1978.
[91] K. Wakino *et al.*, "Quarter wave dielectric transmission line deplexer for land mobile communications," in *1979 IEEE MTT-S Int. Microwave Symp. Dig.*, pp. 278–280, June 1979.
[92] K. Wakino *et al.*, "Miniaturized band pass filters using half wave dielectric resonators with improved spurious response," in *1979 IEEE MTT-S Int. Microwave Symp. Dig.*, pp. 230–232, May 1979.

Oscillator Applications

[93] W. R. Day, "MIC diode oscillator stabilized by a dielectric resonator," in *Proc. 3rd Biennial Cornell Electrical Eng. Conf. in High Frequency Generation and Amplification Device Applications*, Aug. 1971.
[94] G. Satoh, "Stabilized microstrip oscillator using a temperature stable dielectric resonator," in *Dig. IEEE Int. Solid State Circuits Conf.*, pp. 184–185, Feb. 1974.
[95] R. Knochel and K. Schunemann, "Design of cavity-stabilized microwave oscillators," *Electron. Lett.*, pp. 405–406, Aug. 1975.
[96] R. Knochel, K. Schunemann, and J. D. Buchs, "Theory and performance of cavity stabilized microwave oscillators," *Microwaves, Opt. Acoust.*, pp. 143–155, July 1977.
[97] H. Abe *et al.*, "A stabilized low-noise GaAs FET integrated oscillator with a dielectric resonator at C-band," in *IEEE-ISSCC Dig. Tech. Papers*, pp. 168–169, vol. X, Feb. 1977.
[98] H. Abe *et al.*, "Stabilized C-band GaAs FET oscillator," *Microwave J.*, vol. 20, pp. 52–55, Oct. 1977.
[99] H. Abe *et al.*, "A highly stabilized low-noise GaAs FET integrated oscillator with a dielectric resonator in the C band," *IEEE Trans. Microwave Theory Tech.*, vol. MTT-26, pp. 156–162, Mar. 1978.
[100] J. K. Plourde *et al.*, "A dielectric resonator oscillator with 5 ppm long term stability at 4 GHz," in *1977 IEEE MTT-S Int. Microwave Symp. Dig.*, pp. 273–276, June 1977.
[101] J. Sone and Y. Takayama, "A 7 GHz common-drain GaAs FET oscillator stabilized with a dielectric resonator," *NEC Res. Develop. J.*, no. 49, Apr. 1978.
[102] S. Shinozaki, T. Hayasaka, and K. Sakamoto, "6-12 GHz transmission type dielectric resonator transistor oscillators," in *1978 IEEE MTT-S Int. Microwave Symp. Dig.*, pp. 294–299, June 1978.
[103] P. Laesrtre *et al.*, "Stable FET local oscillator at 11 GHz with electronic amplitude control," in *Proc. 8th European Microwave Conf.*, pp. 264–268, Sept. 1978.
[104] S. Watanabe, N. Kusama, and K. Sakamoto, "Very high-Q dielectric resonator voltage-controlled oscillators," in *Proc. 8th European Microwave Conf.*, pp. 269–273, Sept. 1978.
[105] T. Makino, "Temperature dependence and stabilization conditions of an MIC Gunn oscillator using a dielectric resonator," *Trans. IECE Japan*, vol. E62, pp. 262–263, Apr. 1979.
[106] G. D. Alley and H. C. Wang, "An ultra low noise microwave synthesizer," *IEEE Trans. Microwave Theory Tech.*, vol. MTT-27, pp. 969–974, Dec. 1979.
[107] T. Saito *et al.*, "A 6 GHz highly stabilized GaAs FET oscillator using a dielectric resonator," in *1979 IEEE MTT-S Int. Microwave Symp. Dig.*, pp. 197–199, May 1979.
[108] I. Tatsuguchi, D. F. Linn, and W. G. Robinson, "An integrated 18 GHz receiver front end using a dielectric resonator stabilized generator and a subharmonically pumped mixer," in *ICC '79 Conf. Rec.*, pp. 26.2.1–26.2.5, May 1979.
[109] T. Mori *et al.*, "A highly stabilized GaAs FET oscillator using a dielectric resonator feedback circuit in 9-14 GHz," in *1980 IEEE MTT-S Int. Microwave Symp. Dig.*, pp. 376–378, May 1980.
[110] O. Ishihara *et al.*, "DRF-FET oscillator challenges Gunns," *Microwave Syst. News*, pp. 68–70, Feb. 1980.
[111] O. Ishihara *et al.*, "A highly stabilized GaAs FET oscillator using a dielectric resonator feedback circuit in 9-14 GHz," *IEEE Trans. Microwave Theory Tech.*, vol. MTT-28, pp. 817–824, Aug. 1980.
[112] S. J. Greenhalgh *et al.* "Receivers evolving for TV-by-satellite," *Microwave Syst. News*, vol. 10, pp. 82–92, Sept. 1980.

A Reflection Coefficient Approach to the Design of One-Port Negative Impedance Oscillators

DANIEL J. ESDALE AND MICHAEL J. HOWES

***Abstract*—A technique for analyzing microwave oscillators is presented which utilizes readily available device and circuit reflection coefficient information to predict oscillation conditions, stability, and noise performance. The flowgraph approach used yields simple equations which may be readily applied in practice. A graphical interpretation is presented which emphasizes the ease of application of the method proposed.**

Manuscript received November 4, 1980; revised March 12, 1981. This work was supported by the Department of Education of Northern Ireland and Microwave Associates, Dunstable.

The authors are with the Department of Electrical and Electronic Engineering, the University of Leeds, Leeds, England LS29JT.

INTRODUCTION

IN 1969 Kurokawa [1] published a generalized analysis of negative-resistance oscillators. This work provided the basic ideas utilized by others in subsequent analyses, and provided the stimulation for this work.

0018-9480/81/0800-0770$00.75 ©1981 IEEE

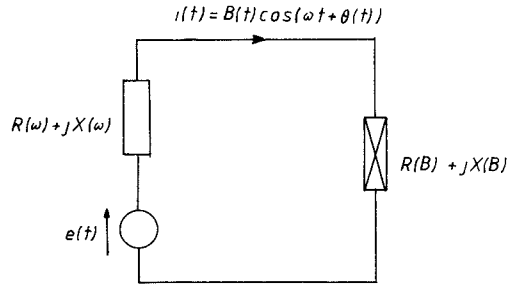

Fig. 1. Oscillator model proposed by Kurokawa.

Kurokawa postulated that if a current waveform

$$i(t)=B(t)\cos(\omega t+\theta(t)) \tag{1}$$

flowed through an impedance then the voltage developed across it may be given as

$$v=\mathrm{Re}\{IZ(\omega')\} \tag{2}$$

where I is the notation of $i(t)$ in the form $Be^{j(\omega t+\theta)}$ and $Z(\omega')$ is the frequency-domain representation of the impedance with functional dependence on a transformed frequency variable

$$\omega'=\omega+\frac{d\theta}{dt}-j\frac{1}{B}\frac{dB}{dt}. \tag{3}$$

$B(t)$ and $\theta(t)$ are assumed to be slowly varying functions of time and may be interpreted as noise modulations in amplitude and phase of the signal at frequency ω.

For the situation depicted in Fig. 1 with device parameters which are time-averaged functions of signal amplitude only ($R(B)$, $X(B)$) and circuit parameters which are solely frequency dependent ($R(\omega)$, $X(\omega)$), differential equations in $B(t)$ and $\theta(t)$ were formulated. Conditions on the interrelation between the device and circuit parameters necessary for oscillation were derived as

$$\begin{aligned} R(\omega)+R(B)&=0\\ X(\omega)+X(B)&=0 \end{aligned} \tag{4}$$

where for a negative impedance device $R(B)$ will be a negative quantity. The oscillations at frequency ω_0 and amplitude B_0 will be stable if and only if

$$\frac{dR}{dB}\Big|_{B_0}\frac{dX}{d\omega}\Big|_{\omega_0}-\frac{dX}{dB}\Big|_{B_0}\frac{dR}{d\omega}\Big|_{\omega_0}>0. \tag{5}$$

Further the frequency spectra of the amplitude-modulation noise and phase-modulation noise are given as

$$|\delta B(\omega)|^2=\frac{2|Z'(\omega_0)|^2|e|^2}{\omega^2|Z'(\omega_0)|^4+\left(\frac{dR}{dB}\frac{dX}{d\omega}-\frac{dX}{dB}\frac{dR}{d\omega}\right)^2|B_0|^2} \tag{6}$$

$$|\delta\theta(\omega)|^2=\frac{2|e|^2}{\omega^2|B_0|^2}\cdot\frac{\omega^2|Z'(\omega_0)|^2+|B_0|^2\left[\left(\frac{dR}{dB}\right)^2+\left(\frac{dX}{dB}\right)^2\right]}{\omega^2|Z'(\omega_0)|^4+\left(\frac{dR}{dB}\frac{dX}{d\omega}-\frac{dX}{dB}\frac{dR}{d\omega}\right)^2|B_0|^2} \tag{7}$$

where $|e|^2$ is the squared magnitude of the intrinsic white-noise generator and

$$|Z'(\omega_0)|^2=\left[\left(\frac{dR}{d\omega}\right)^2+\left(\frac{dX}{d\omega}\right)^2\right]_{|\omega_0}. \tag{8}$$

These expressions have proved to be useful in first-order oscillator analysis. However, this approach utilizes voltage, current, and impedances all of which may not be directly measured at microwave frequencies. In this paper, a similar theory in terms of incident and reflected traveling waves and scattering parameters is developed. It is felt that in addition to utilizing measurable microwave quantities, the method developed here, essentially a flowgraph approach, is more amenable to extension to more complicated oscillator structures and is presently being refined to investigate noise aspects in GaAs MESFET oscillators.

Flow Graph Method

To utilize a flowgraph approach, we define a normalized wave sinusoidal in space and time incident on an arbitrary impedance, Z, in terms of the phasor voltage and current across and through Z

$$a=\tfrac{1}{2}\left(\frac{V}{\sqrt{Z_0}}+I\sqrt{Z_0}\right). \tag{9}$$

Similarly, the reflected wave may be defined

$$b=\tfrac{1}{2}\left(\frac{V}{\sqrt{Z_0}}-I\sqrt{Z_0}\right) \tag{10}$$

where the ratio of b to a is the reflection coefficient, Γ, of the impedance. Employing (9) and (10) we find the usual relationship for Γ as

$$\Gamma=\frac{Z-Z_0}{Z+Z_0}. \tag{11}$$

This linear transformation between $Z(\omega)$ and $\Gamma(\omega)$ will continue to hold when the functional dependence of $Z(\omega)$ is altered due to the nonsinusoidal current (1). However, the linear relationship between a, b, V, I through (9) and (10) suggests that we may represent the time-domain incident wave in the form

$$a(t)=A(t)\cos[\omega t+\phi(t)] \tag{12}$$

and we postulate that the reflected wave may be given by a "circuit law" analogous to (2)

$$b(t)=\mathrm{Re}\left[Ae^{j(\omega t+\phi)}\cdot\Gamma\left(\omega+\frac{d\phi}{dt}-j\frac{1}{A}\frac{dA}{dt}\right)\right]. \tag{13}$$

Note that we modify the functional dependence of $\Gamma(\omega)$ to

$$\Gamma\left(\omega+\frac{d\phi}{dt}-j\frac{1}{A}\frac{dA}{dt}\right)$$

and *not* to

$$\Gamma\left(\omega+\frac{d\theta}{dt}-j\frac{1}{B}\frac{dB}{dt}\right).$$

This basic postulate will now be employed to develop an analysis of an oscillator comprising a frequency-invariant active device and a generalized circuit with reflection coefficient Γ_c.

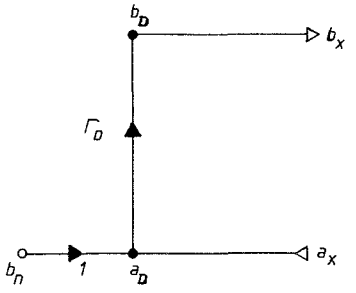

Fig. 2. Flowgraph model of active device including noise wave generator.

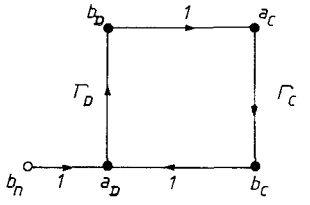

Fig. 3. Flowgraph model of oscillator used in this study.

A single wave generator is introduced which models the noise mechanisms within the active device, this is denoted as b_n in Fig. 2.

The total wave incident on the device is given as

$$a_D = a_x + b_n \tag{14}$$

and the reflected wave

$$b_x = b_D = \Gamma_D(a_x + b_n) \tag{15}$$

i.e.,

$$b_D = \Gamma_D a_D. \tag{16}$$

Now if the total wave incident on the device is represented as

$$a_D(t) = A(t)\cos[\omega t + \phi(t)] \tag{17}$$

then we postulate that the device reflection coefficient which relates b_D to a_D is a time-averaged function of the amplitude A and is denoted as $\Gamma_D(A)$.

As the signal amplitude, A, increases then the level of harmonics in b_D will increase. However, we may continue to define a linear operator $\Gamma_D(A)$ which relates the fundamental component of b_D to a fundamental component of a_D. If the device is loaded with a reflection coefficient which is nonzero at its fundamental and harmonic frequencies then the returned incident wave a_D will contain harmonic components. The linear operator, Γ_D, relating the fundamental component in b_D to the fundamental in a_D is then a function of the time-averaged amplitudes of the fundamental and all-harmonic components in a_D. In this analysis, we assume that the device is loaded by a reflection coefficient of zero, i.e., terminated in Z_0 at all harmonic frequencies.

If we couple the device and noise generator to the circuit of Fig. 3 then

$$a_D = b_n + \Gamma_c b_c \tag{18}$$

$$a_D = b_n + \Gamma_c \Gamma_D a_D \tag{19}$$

the total wave incident on the device in the "closed-loop" regime is given by

$$a_D[1 - \Gamma_c(\omega)\Gamma_D(A)] = b_n \tag{20}$$

assuming the amplitudes of the harmonics are small.

If a quasi-sinusoidal waveform for $a_D(t)$ is assumed which is noise modulated in phase and amplitude, we must modify the system equation to include (13). This procedure gives

$$\mathrm{Re}\left\{Ae^{j(\omega t+\phi)}\left[1 - \Gamma_D(A)\Gamma_c\left(\omega + \frac{d\phi}{dt} - j\frac{1}{A}\frac{dA}{dt}\right)\right]\right\} = b_n(t). \tag{21}$$

If the investigation is restricted to cases in which $d\phi/dt \ll \omega$ and $(1/A)(dA/dt) \ll \omega$, normally valid except in transient situations, the circuit reflection coefficient may be expanded and then truncated to the first term in a Taylor series, thus

$$\Gamma_c(\omega) + \frac{d\Gamma_c(\omega)}{d\omega}\left[\frac{d\phi}{dt} - j\frac{1}{A}\frac{dA}{dt}\right]. \tag{22}$$

Since reflection coefficients are normally represented in polar form we may define

$$\Gamma_c(\omega) = \eta(\omega)e^{j\xi(\omega)} \tag{23}$$

$$\Gamma_D(A) = \rho(A)e^{j\theta(A)} \tag{24}$$

then

$$\frac{d\Gamma_c}{d\omega} = e^{j\xi}\left[\frac{d\eta}{d\omega} + j\eta\frac{d\xi}{d\omega}\right]. \tag{25}$$

The "closed-loop" equation (21) is modified to

$$\begin{aligned}
&A\cos(\omega t+\phi)\left[1 - \rho\cos(\theta+\xi)\left(\eta + \frac{d\eta}{d\omega}\frac{d\phi}{dt} + \eta\frac{d\xi}{d\omega}\frac{1}{A}\frac{dA}{dt}\right)\right.\\
&\left. + \rho\sin(\theta+\xi)\left(\eta\frac{d\xi}{d\omega}\frac{d\phi}{dt} - \frac{d\eta}{d\omega}\frac{1}{A}\frac{dA}{dt}\right)\right]\\
&+ A\sin(\omega t+\phi)\left[\rho\sin(\theta+\xi)\left(\eta + \frac{d\eta}{d\omega}\frac{d\phi}{dt} + \eta\frac{d\xi}{d\omega}\frac{1}{A}\frac{dA}{dt}\right)\right.\\
&\left. + \rho\cos(\theta+\xi)\left(\eta\frac{d\xi}{d\omega}\frac{d\phi}{dt} - \frac{d\eta}{d\omega}\frac{1}{A}\frac{dA}{dt}\right)\right]\\
&= b_n(t).
\end{aligned} \tag{26}$$

We may remove the high-frequency and harmonic dependence to investigate the modulations by multiplying by $\cos(\omega t+\phi)$ and integrating over one period, T_0, and similarly with $\sin(\omega t+\phi)$. This yields two coupled differential equations

$$P - Q\frac{d\phi}{dt} - R\frac{1}{A}\frac{dA}{dt} = n_A \tag{27}$$

$$S - R\frac{d\phi}{dt} - Q\frac{1}{A}\frac{dA}{dt} = n_B. \tag{28}$$

The coefficients are

$$\begin{aligned}
P &= 1 - \rho\eta\cos(\theta+\xi)\\
S &= \rho\eta\sin(\theta+\xi)\\
Q &= \rho\cos(\theta+\xi)\frac{d\eta}{d\omega} - \rho\eta\sin(\theta+\xi)\frac{d\xi}{d\omega}\\
R &= \rho\sin(\theta+\xi)\frac{d\eta}{d\omega} + \rho\eta\cos(\theta+\xi)\frac{d\xi}{d\omega}
\end{aligned} \tag{29}$$

and

$$n_A = \frac{2}{A}\frac{1}{T_0}\int_t^{t+T_0} b_n(t)\cos(\omega t+\phi)\,dt$$

$$n_B = \frac{2}{A}\frac{1}{T_0}\int_t^{t+T_0} b_n(t)\sin(\omega t+\phi)\,dt \tag{30}$$

where n_A and n_B are orthogonal noise components such that $n_A n_B^* = n_A^* n_B = 0$.

Oscillation Conditions

When we place the noise source to zero and investigate the steady-state situation, i.e., dA/dt and $d\phi/dt$, both zero in (27) and (28), then

$$1-\rho\eta\cos(\theta+\xi)=0$$
$$\rho\eta\sin(\theta+\xi)=0. \tag{31}$$

These conditions are simultaneously satisfied if

$$\theta=-\xi$$

and

$$\rho=1/\eta. \tag{32}$$

From the definitions (23) and (24) we identify the requirement

$$\Gamma_c=1/\Gamma_D \tag{33}$$

for steady-state oscillation.

Stability Conditions

The stability of any oscillation may be investigated by perturbing the amplitude and phase about the operating amplitude, A_0, and frequency, ω_0, and noting if the perturbation decays with time or shifts to some other valid but stable operating point, ω_1, A_1. If the amplitude is perturbed by δA then the device parameters at $(A_0+\delta A)$ may be given by a linear approximation, the first terms in a Taylor series expansion about the operating point

$$\Gamma_D(A_0+\delta A)=\Gamma_D(A_0)+\frac{d\Gamma_D}{dA}\delta A$$
$$=\rho e^{j\theta}+e^{j\theta}\left[\frac{d\rho}{dA}+j\rho\frac{d\theta}{dA}\right]\delta A. \tag{34}$$

The coefficients in the differential equations (27) and (28) are modified due to this change and in particular we replace $\rho\cos\theta$ by

$$\rho\cos\theta+\left[\frac{d\rho}{dA}\cos\theta-\rho\frac{d\theta}{dA}\sin\theta\right]\delta A \tag{35}$$

and $\rho\sin\theta$ by

$$\rho\sin\theta+\left[\frac{d\rho}{dA}\sin\theta+\rho\frac{d\theta}{dA}\cos\theta\right]\delta A. \tag{36}$$

Utilizing this and the oscillation conditions (31) which exist at ω_0, A_0 it can be shown that the coefficients in the differential equations become

$$P'=-\eta\frac{d\rho}{dA}\delta A$$

$$S'=\frac{d\theta}{dA}\delta A$$

and

$$Q'=\rho\frac{d\eta}{d\omega}+\left[\frac{d\eta}{d\omega}\frac{d\rho}{dA}-\frac{d\xi}{d\omega}\frac{d\theta}{dA}\right]\delta A$$

$$R'=\frac{d\xi}{d\omega}+\left[\rho\frac{d\eta}{d\omega}\frac{d\theta}{dA}+\eta\frac{d\xi}{d\omega}\frac{d\rho}{dA}\right]\delta A. \tag{37}$$

Differential equations in δA and $\delta\phi$ alone may be obtained from (27) and (28).

$$(R'P'+Q'S')-(R'^2+Q'^2)\frac{1}{A_0}\frac{d(\delta A)}{dt}=R'n_A+Q'n_B \tag{38}$$

$$(Q'P'-R'S')-(R'^2+Q'^2)\frac{d(\delta\phi)}{dt}=Q'n_A-R'n_B. \tag{39}$$

Since $(R'^2+Q'^2)$ is always positive then the amplitude perturbation will decay if

$$R'P'+Q'S'<0. \tag{40}$$

Thus we require that the device and circuit have parameters which fulfill

$$\eta\frac{d\rho}{dA}\frac{d\xi}{d\omega}-\rho\frac{d\theta}{dA}\frac{d\eta}{d\omega}>0 \tag{41}$$

at the operating point ω_0, A_0 if any oscillation predicted by (33) is to be stable.

Graphical Interpretation

Kurokawa [1] and Kenyon [2] provided a graphical insight into the oscillation stability and noise performance derived by Kurokawa. They primarily investigated the intersection of the impedance locus of the circuit as a function of frequency with the negative of the impedance locus of the device with amplitude as parameter, (see Fig. 4).

In the reflection coefficient plane, a negated impedance is equivalent to the inverse reflection coefficient. We, therefore, explore the intersection of the locus of the circuit reflection coefficient Γ_c with the inverse locus of the device reflection coefficient Γ_D.

It is true that the conditions which we derive below could be trivially arrived at by employing Kurokawa and Kenyon results and invoking the angle preserving nature of the conformal mapping which relates $\Gamma(\omega)$ to $Z(\omega)$, (11). However, this approach would investigate stability of the current waveform within the circuit by exploring δB and $\delta\theta$, see (1). Now, since the wave, a, is linearly related to this current through (9) then stability of current oscillation and conditions for minimum current noise will correspond to stable wave oscillation and minimum noise thereof.

The method here which explores stability and noise performance of the wave through δA and $\delta\phi$ yields graphical interpretation which agrees with those derived by invoking the conformal-mapping argument discussed above. This check gives some confidence in this new approach and justification for further development of this theory.

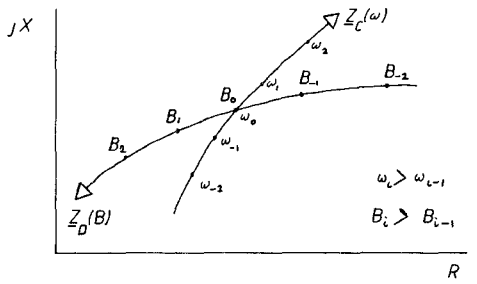

Fig. 4. Circuit impedance locus as a function of frequency and negated device impedance locus as a function of signal amplitude.

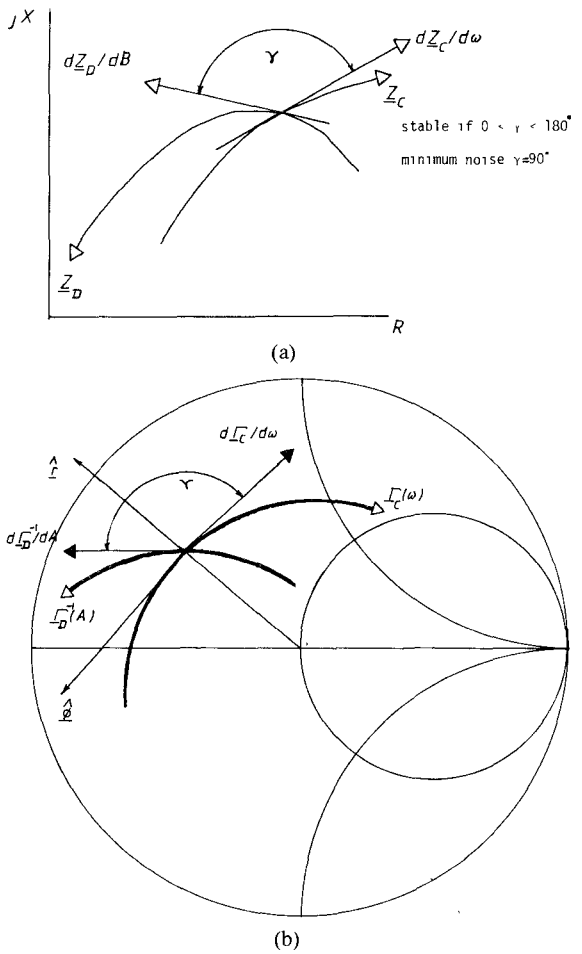

Fig. 5. (a) Conditions on the intersection of the circuit and device loci in the Z-plane. (b) Circuit locus and *inverse* device locus in the reflection coefficient plane.

Fig. 5(a) represents the loci intersection in the Z-plane and indicates the conditions necessary for stability of oscillation at ω_0, B_0 and conditions for minimum noise performance. Fig. 5(b) investigates the intersection of equivalent loci expressed as vectors in the reflection coefficient plane. Denoting the inverse device reflection coefficient as

$$\Gamma_D^{-1} = re^{j\Omega} \tag{42}$$

where

$$\begin{aligned} r &= 1/\rho \\ \Omega &= -\theta \end{aligned} \tag{43}$$

we may transform the stability condition (41) by noting

$$\frac{d\rho}{dA} = \frac{d\rho}{dr}\frac{dr}{dA} \quad \text{and} \quad \frac{d\theta}{dA} = \frac{d\theta}{d\Omega}\frac{d\Omega}{dA}$$
$$= -\frac{1}{r^2}\frac{dr}{dA} \qquad = -\frac{d\Omega}{dA} \tag{44}$$

$\therefore$

$$\frac{dr}{dA}\frac{d\xi}{d\omega} - \frac{d\eta}{d\omega}\frac{d\Omega}{dA} < 0. \tag{45}$$

We identify these terms as cross coupling of the components of the vectors which are tangential to the circuit and device loci at the operating point. If we represent these vectors in a cylindrical coordinate system as

$$\frac{d(\Gamma_c)}{d\omega} = \frac{d\eta}{d\omega}\hat{r} + \frac{d\xi}{d\omega}\hat{\phi} + 0\hat{z} \tag{46}$$

$$\frac{d(\Gamma_D^{-1})}{dA} = \frac{dr}{dA}\hat{r} + \frac{d\Omega}{dA}\hat{\phi} + 0\hat{z} \tag{47}$$

then, in fact, we identify (45) as

$$\frac{d(\Gamma_c)}{d\omega} \times \frac{d(\Gamma_D^{-1})}{dA} > 0 \tag{48}$$

since the compact form of cross product

$$\frac{d(\Gamma_c)}{d\omega} \times \frac{d(\Gamma_D^{-1})}{dA} = \begin{vmatrix} \hat{r} & \hat{\phi} & \hat{z} \\ d\eta/d\omega & d\xi/d\omega & 0 \\ dr/dA & d\Omega/dA & 0 \end{vmatrix}$$
$$= \left|\frac{d(\Gamma_c)}{d\omega}\right| \left|\frac{d(\Gamma_D^{-1})}{dA}\right| \sin\gamma \tag{49}$$

may be employed. This is because

$$\frac{d(\Gamma_c)}{d\omega} \quad \text{and} \quad \frac{d(\Gamma_D^{-1})}{dA}$$

are fixed vectors operating through the same point and the orientation of the unit vectors is the same, at that point in space, for Γ_c, Γ_D^{-1}, and their resultant product.

Thus we identify stable oscillation as $\sin\gamma > 0$, i.e., $0 < \gamma < 180°$ which may be compared with Fig. 5(a).

Noise Analysis

If in (38) and (39) we identify the perturbations $\delta A, \delta\phi$ as amplitude-modulated and phase-modulated noise generated by the interaction of $b_n(t)$ with the circuit and device we may solve for the noise spectra of the overall oscillator.

Modifying (38) and (39) to include the inverse device reflection coefficient parameters we now identify

$$(R'^2 + Q'^2) = \left(\frac{1}{\eta}\frac{d\eta}{d\omega}\right)^2 + \left(\frac{d\xi}{d\omega}\right)^2 \tag{50}$$

and

$$\frac{d(\Gamma_c)}{d\omega} = \eta e^{j\xi}\left[\frac{1}{\eta}\frac{d\eta}{d\omega} + j\frac{d\xi}{d\omega}\right] \tag{51}$$

$$\left|\frac{d\Gamma_c}{d\omega}\right|^2 = |\eta|^2\left[\left(\frac{1}{\eta}\frac{d\eta}{d\omega}\right)^2 + \left(\frac{d\xi}{d\omega}\right)^2\right] \tag{52}$$

whence

$$(R'^2+Q'^2)=\frac{1}{\eta^2}\left|\frac{d(\Gamma_c)}{d\omega}\right|^2. \tag{53}$$

Further

$$(R'P'+Q'S')=\frac{1}{\eta}\left[\frac{d\xi}{d\omega}\frac{dr}{dA}-\frac{d\Omega}{dA}\frac{d\eta}{d\omega}\right]\delta A \tag{54}$$

$$(Q'P'-R'S')=\left[\frac{1}{\eta^2}\frac{dr}{dA}\frac{d\eta}{d\omega}+\frac{d\xi}{d\omega}\frac{d\Omega}{dA}\right]\delta A. \tag{55}$$

Thus (38) and (39) become

$$A_0\frac{1}{\eta}\left[\frac{d\xi}{d\omega}\frac{dr}{dA}-\frac{d\Omega}{dA}\frac{d\eta}{d\omega}\right]\delta A-\frac{1}{\eta^2}\left|\frac{d(\Gamma_c)}{d\omega}\right|^2\frac{d(\delta A)}{dt}=[R'n_A+Q'n_B]A_0 \tag{56}$$

$$\left[\frac{1}{\eta^2}\frac{dr}{dA}\frac{d\eta}{d\omega}+\frac{d\xi}{d\omega}\frac{d\Omega}{dA}\right]\delta A-\frac{1}{\eta^2}\left|\frac{d(\Gamma_c)}{d\omega}\right|^2\frac{d(\delta\phi)}{dt}=Q'n_A-R'n_B. \tag{57}$$

Taking the Fourier transform of (56), rearranging, and examining the modulus squared

$$|\delta A(\omega)|^2=\frac{|A_0|^2|R'n_A+Q'n_B|^2}{|A_0|^2\frac{1}{\eta^2}\left(\frac{d\xi}{d\omega}\frac{dr}{dA}-\frac{d\Omega}{dA}\frac{d\eta}{d\omega}\right)^2+\frac{1}{\eta^4}\left|\frac{d\Gamma_c}{d\omega}\right|^4\omega^2}. \tag{58}$$

Now

$$\begin{aligned}|R'n_A+Q'n_B|^2&=(R'n_A+Q'n_B)(R'^*n_A^*+Q'^*n_B^*)\\&=R'^2|n_A|^2+Q'^2|n_B|^2\end{aligned} \tag{59}$$

since

$$n_An_B^*=n_A^*n_B=0.$$

Also

$$|n_A|^2=|n_B|^2=2|b_n|^2/|A_0|^2$$

where $|b_n|^2$ may be related to Kurokawa's noise generator $|e|^2$ as

$$|b_n|^2=|e|^2|1-\Gamma_D|^2/4Z_0|\Gamma_D|^2.$$

The amplitude-modulated noise spectrum at the modulation frequency, ω_m, is

$$|\delta A(\omega_m)|^2=\frac{\frac{1}{\eta^2}\left|\frac{d\Gamma_c}{d\omega}\right|^2 2|b_n|^2}{|A_0|^2\frac{1}{\eta^2}\left(\frac{d\xi}{d\omega}\frac{dr}{dA}-\frac{d\Omega}{dA}\frac{d\eta}{d\omega}\right)^2+\frac{1}{\eta^4}\left|\frac{d\Gamma_c}{d\omega}\right|^4\omega_m^2} \tag{60}$$

where (53) has been employed to simplify the numerator. Employing (49), the denominator may be simplified yielding

$$|\delta A(\omega_m)|^2=\frac{\frac{1}{\eta^2}\left|\frac{d\Gamma_c}{d\omega}\right|^2 2|b_n|^2}{|A_0|^2\frac{1}{\eta^2}\left|\frac{d\Gamma_c}{d\omega}\times\frac{d\Gamma_D^{-1}}{dA}\right|^2+\frac{1}{\eta^4}\left|\frac{d\Gamma_c}{d\omega}\right|^4\omega_m^2}. \tag{61}$$

From this equation we note that the amplitude-modulated noise spectrum is a function of the vectors tangential to the circuit and inverse device loci. Indeed, the interaction between the device and circuit reflection coefficients will produce a minimum in the amplitude-modulated noise spectrum at all modulation frequencies when the tangential vectors intersect orthogonally; this is identical to the condition derived by Kurokawa and Kenyon for the impedance loci.

To investigate the phase noise spectrum we take the Fourier transform of (57) which yields after rearrangement, squaring of the modulus, substitution of (58), (59), and noting that the coefficients of Q' and R' are wholly real

$$|\delta\phi(\omega_m)|^2=\frac{2|b_n|^2}{\omega_m^2|A_0|^2}\cdot\frac{\frac{1}{\eta^2}\left|\frac{d\Gamma_D^{-1}}{dA}\right|^2|A_0|^2+\frac{1}{\eta^2}\left|\frac{d\Gamma_c}{d\omega}\right|^2\omega_m^2}{|A_0|^2\frac{1}{\eta^2}\left|\frac{d\Gamma_c}{d\omega}\times\frac{d\Gamma_D^{-1}}{dA}\right|^2+\frac{1}{\eta^4}\left|\frac{d\Gamma_c}{d\omega}\right|^4\omega_m^2} \tag{62}$$

where we have also employed

$$\left|\frac{d\Gamma_D^{-1}}{dA}\right|^2=\eta^2\left[\left(\frac{1}{\eta}\frac{dr}{dA}\right)^2+\left(\frac{d\Omega}{dA}\right)^2\right]. \tag{63}$$

Equation (62) indicates that the phase noise spectrum depends on the vectors tangential to the circuit and device loci in a similar manner to the amplitude-modulated noise. The numerator in this expression is slightly more complicated but, in general, good noise performance may be achieved if

i) the circuit and inverse device loci intersect orthogonally

ii) the value of $\left|\frac{1}{\eta}\frac{d(\Gamma_c)}{d\omega}\right|$ is maximized

iii) the value of $\left|\frac{1}{\eta}\frac{d(\Gamma_D)^{-1}}{dA}\right|$ is minimized.

Conclusions

In this paper we have developed a first-order one-port negative resistance oscillator analysis utilizing the traveling-wave concept and employing a reflection coefficient description of the active device and circuit elements. This approach has been undertaken since reflection coefficient information is more readily available from manufacturers data sheets or in presently available instrumentation sys-

tems at microwave frequencies rather than impedance data. Further, a wave approach to the problem enables more complicated oscillator structures to be investigated through the relatively easy application of Mason's topological rules to the flowgraph description.

From the investigation of a mildly nonlinear device/circuit interaction such that noise modulations pass linearly around the oscillator we have derived formulas for oscillation condition and stability. Expressions for the amplitude and phase noise of the oscillator have also been derived. A graphical interpretation of these conditions has been presented in terms of the circuit reflection coefficient and inverse device reflection coefficient loci in a cylindrical coordinate system. The results of this graphical investigation have been shown to be equivalent to those derived by Kurokawa.

References

[1] K. Kurokawa, "Some basic characteristics of broadband negative resistance oscillator circuits," *Bell syst. Tech. J.*, vol. 48, no. 6, pp. 1937–1955, July 1969.

[2] N. D. Kenyon, "A lumped-circuit study of basic oscillator behavior," *Bell Syst. Tech. J.*, vol. 49, no. 2, pp. 255–272, Feb. 1970.

RF Characterization of Microwave Power FET's

RODNEY S. TUCKER, MEMBER, IEEE

Abstract— **The large-signal S-parameter S_{22} and the optimum load for maximum output power are two parameters commonly used in the RF characterization of microwave power FET's. Using a nonlinear circuit model of the device, the dependence on RF power of each of these parameters is investigated. A method is given for computing the optimum load from the large-signal S_{22}. Equivalent load-pull data can thus be obtained without the need for load-pull measurements. The gain compression characteristics of the transistor for arbitrary load can be computed from large-signal S_{21} and S_{22} data.**

I. Introduction

IN THE ANALYSIS and design of GaAs FET power amplifiers there is a need for data on device RF characteristics at large-signal levels. Experimental methods for obtaining these data fall into two main classes: large-signal S-parameter measurements [1], [2] and load-pull measurements [3]–[7]. Large-signal S-parameters are an extension of the well-known small-signal S-parameters [8] and are generally measured with fixed 50-Ω terminations at the device terminals. Load-pull measurements differ from large-signal S-parameter measurements in that the terminations are not held constant. The device is driven at a given input power level and parameters such as output power [3] or intermodulation distortion [7] are measured as a function of the load admittance. A load-pull parameter which is particularly useful in the design of power-amplifiers is the *optimum load admittance for maximum output power* [3], [4].

The variable load admittance used in load-pull measurements can be set up either using a tuner [3], [6] or with a second signal injected at the output port of the device [4], [5], [7]. Both of these loading techniques give circuit conditions which closely resemble those the FET will experience in an amplifier. Therefore, the main advantage of load-pull data over large-signal S-parameter data is that they are measured under realistic operating conditions. As a result, load-pull data are well suited to analysis and design procedures.

Large-signal S-parameter measurements are generally easier and less tedious to implement than load-pull measurements. In addition, large-signal S-parameters can be readily measured on a swept-frequency basis. Unfortunately, large-signal S-parameters are less useful than load-pull data in circuit analysis and design. This problem arises because small-signal S-parameters (and thus large-signal S-parameters) are defined in terms of a *linear* two-port network [8]. Under large-signal conditions, a microwave transistor is nonlinear and large-signal S-parameters cannot be used to predict the large-signal device performance for terminations other than the fixed terminations used during measurement. In addition, it is not clear what signal power level should be used for large-signal S-parameter measurements.

Manuscript received July 28, 1980; revised March 5, 1981. This work was supported by Telecom Australia, the Australian Radio Research Board, and the Australian Research Grants Committee.

The author is with the Department of Electrical Engineering, University of Queensland, St. Lucia, Brisbane, Qld. 4067, Australia.

0018-9480/81/0800-0776$00.75 ©1981 IEEE